韓國水資源學會論文集
第34卷 第2號 · 2001年 4月
pp. 169~176

Numerical Simulation of Transoceanic Propagation and Run-up of Tsunami

지진해일의 전파와 처오름에 관한 수치해석

Cho, Yong-Sik* / Yoon, Sung Bum**
조 용 식 / 윤 성 범

Abstract

The propagation and associated run-up process of tsunami are numerically investigated in this study. A transoceanic propagation model is first used to simulate the distant propagation of tsunamis. An inundation model is then employed to simulate the subsequent run-up process near coastline. A case study is done for the 1960 Chilean tsunami. A detailed maximum inundation map at Hilo Bay is obtained and compared with field observation and other numerical model predictions. A very reasonable agreement is observed.

keywords : tsunami, shallow-water equations, propagation, run-up, inundation map

요 지

지진해일의 전파와 이에 부수되는 처오름과정에 관한 수치해석에 관하여 연구하였다. 먼저, 대양을 가로질러 전파하는 지진해일을 모의하는 전파모형과 해안선 근처에서의 처오름과정을 모의하는 범람모형에 대하여 서술하였다. 수치모형을 1960년 칠레 지진해일에 적용하여 지진해일의 전파과정과 하와이 힐로만에서의 범람을 수치해석하였다. 힐로만의 최대범람구역을 결정하여 현장관측자료 및 다른 수치해석 예측과 비교하여 매우 만족할만한 결과를 얻었다.

핵심용어 : 지진해일, 천수방정식, 전파, 처오름, 범람도

* 한양대학교 공과대학 토목공학과 조교수
Assistant Professor, Department of Civil Engineering, Hanyang University, Seoul 133-791, Korea
(E-mail : ysc59@hanyang.ac.kr)
** 한양대학교 공학대학 토목환경공학과 부교수
Associate Professor, Department of Civil and Environmental Engineering, Hanyang University, Kyeonggi 425-791, Korea (E-mail : sbyoon@hanyang.ac.kr)

1. Introduction

Because of characteristics of long waves, tsunamis may cause serious damage not only in those countries located near the earthquake source but also in the countries far from the source after a long journey even across an ocean. Among more than 100 tsunamis observed in the Pacific Ocean Area during the last century, the Chilean tsunami occurred in 1960 was recorded probably as the most destructive tsunamis(Lander and Lockridge, 1989).

A plausible and practical way for the tsunami hazard mitigation is to construct an inundation map along the coastline liable to tsunami attacks. To produce a realistic and reliable inundation map, it is necessary to use a numerical model simulating accurately tsunami propagation from a source region to the coastal areas of concern and the associated run-up process. Due to requirement of a huge memory size and high speed computing, however, few numerical studies have been reported for the transoceanic propagation and run-up process of tsunamis(e.g., Houston, 1978; Imamura et al., 1988; Mader and Curtis, 1991).

Among them, Houston(1978) studied the interaction of 1960 Chilean and 1964 Alaskan tsunamis with the Hawaiian Islands chain by using a finite element method. Calculated time history of free surface displacement was compared with tidal gage recordings at several locations. A good agreement was observed, but no inundation map was made.

In Imamura et al.'s study(1988), the main interest was the tsunami run-up along the Japanese coastline. Therefore, a coarse grid system was used in the Pacific Ocean; they used a 10min(approximately 18km) grid in the area. No inundation model was used. Thus, the maximum run-up heights were calculated by using Green's law.

On the other hand, Mader and Curtis(1991) used 20min(approximately 36km) and 5min (approximately 9km) grids to simulate the transoceanic propagation of the 1960 Chilean tsunamis across the Pacific Ocean to Hawaii. The tsunami run-up at Hilo Bay was then calculated by using a 100m×100m grid system. Therefore, there was an abrupt change from the large grid system to the small one in the numerical model. The offshore boundary of the small grid system was represented by a single point in the large one. Hence, the boundary condition was always uniform along the offshore boundary.

In this paper, the transoceanic propagation and subsequent run-up process of tsunamis are studied. Especially, the 1960 Chilean tsunami is numerically investigated in detail. The present study provides numerical results with a much finer resolution in the vicinity of the Hawaiian Islands chain than previous studies. Furthermore, a maximum inundation map at Hilo Bay is obtained and compared with field observed data and other predictions. Maximum run-up heights at several locations are also calculated and compared with field recordings.

2. Governing Equations

To model the transoceanic propagation and associated run-up process of tsunamis the adequate governing equations are first presented in this section for completeness. Using a typical wave amplitude of 2m, Cho(1995) estimated the relative importance of nonlinear inertia force, pressure force, Coriolis force, bottom friction and frequency dispersion with respect to the local inertia force. He concluded that nonlinear inertia force and bottom friction are relatively insignificant and may be neglected in modelling of the transoceanic propagation of tsunamis.

Because tsunamis may travel a very long distance from a source region to a target

region, the Coriolis force may be important. Furthermore, the frequency dispersion effects depend on the wavelength and it could be included in the governing equations. Hence, the transoceanic propagation of tsunamis can be adequately described by the linear Boussinesq equations given as

$$\frac{\partial \zeta}{\partial t} + \frac{\partial P}{\partial x} + \frac{\partial Q}{\partial y} = 0 \tag{1}$$

$$\frac{\partial P}{\partial t} + gh\frac{\partial \zeta}{\partial x} - fP = \frac{\partial^2}{\partial t \partial x}\left[\frac{h^3}{3}\left\{\frac{\partial}{\partial x}\left(\frac{P}{h}\right) + \frac{\partial}{\partial y}\left(\frac{Q}{h}\right)\right\}\right] \tag{2}$$

$$\frac{\partial Q}{\partial t} + gh\frac{\partial \zeta}{\partial y} + fQ = \frac{\partial^2}{\partial t \partial y}\left[\frac{h^3}{3}\left\{\frac{\partial}{\partial x}\left(\frac{P}{h}\right) + \frac{\partial}{\partial y}\left(\frac{Q}{h}\right)\right\}\right] \tag{3}$$

where ζ is the free surface displacement, P and Q are the depth-averaged volume flux components in x and y-directions, respectively, h is the still water depth, g is the gravitational acceleration and f is the Coriolis parameter.

Equation (1) is an exact expression of the conservation of mass, while equations (2) and (3) are approximate statements of the conservation of momentum fluxes averaged over the depth. The terms of right-hand side of the momentum equation result from the hydrodynamic pressure force or from the vertical acceleration. These terms modify the dispersion relationship of the linear shallow-water wave system and changes the phase velocity. They are usually referred to as the frequency dispersion terms.

As the tsunami approaches a coastal zone, the wavelength becomes shorter and the amplitude becomes larger as leading waves of a tsunami propagate into shallower water. The nonlinear convective inertia force and the bottom friction terms become increasingly important, whereas the significance of frequency dispersion terms diminishes. The nonlinear shallow-water equations, including bottom frictional effects, are adequate to describe the tsunami inundation in the coastal area(Kajiura and Shuto, 1990). A special treatment is needed along the shoreline to track its movements properly as waves rise and recede(Cho and Liu, 1999).

The governing equations for the flow motions in shallow water can be written as

$$\frac{\partial \zeta}{\partial t} + \frac{\partial P}{\partial x} + \frac{\partial Q}{\partial y} = 0 \tag{4}$$

$$\frac{\partial P}{\partial t} + \frac{\partial}{\partial x}\left(\frac{P^2}{H}\right) + \frac{\partial}{\partial y}\left(\frac{PQ}{H}\right) + gH\frac{\partial \zeta}{\partial x} + \frac{g}{C_f^2 H^2} P(P^2+Q^2)^{1/2} = 0 \tag{5}$$

$$\frac{\partial Q}{\partial t} + \frac{\partial}{\partial x}\left(\frac{PQ}{H}\right) + \frac{\partial}{\partial y}\left(\frac{Q^2}{H}\right) + gH\frac{\partial \zeta}{\partial y} + \frac{g}{C_f^2 H^2} Q(P^2+Q^2)^{1/2} = 0 \tag{6}$$

in which $H=h+\zeta$ is the total depth. In equations (5) and (6), the bottom frictional forces are expressed by using the Chezy's formula with being C_f the frictional coefficient. In this study, the shoreline is defined as the location of zero total depth, i.e. $H=0$.

Detailed descriptions of the numerical schemes for equations (1)-(3) and (4)-(6) can be found in Cho and Yoon(1998) and Cho and Liu(1999), respectively and are not repeated here.

3. Numerical Simulation of Transoceanic Propagation

In this section, the transoceanic propagation of the 1960 Chilean tsunami is simulated by using the governing equations given by (1)-(3) and (4)-(6). The bathymetric data for the Pacific Ocean is generated from the ETOPO5. The ETOPO5 is a gridded data set of land and seafloor elevations of the whole Earth and is made by the National Geophysical Data Center, National Oceanic and Atmospheric Administration, U.S. Department of Commerce.

The epicenter of the 1960 Chilean earthquake is located about 100km offshore of the Chilean coast. The fault zone is roughly 800km long and 200km wide, and the displacement of the fault is 24m. The orientation of the fault is N10oE. The focal depth of the slip is estimated at 53km with a 90o slip angle and a 10o dip angle. The initial free surface displacement can be estimated by using these estimated fault parameters(Manshinha and Smylie, 1971). The wavelength of the initial tsunami form is roughly 1,000km and the wave height is about 10m.

The distance between the Hawaiian Islands chain and the source region of the Chilean tsunami is about 10,000km. Because the average depth in the Pacific Ocean is approximately 4km and the tsunami travels at a speed of approximately 200m/sec, it takes roughly 14 to 15 hours for the leading part of tsunamis to arrive at the Hawaiian Islands chain. Because of the frequency dispersion and spreading of wave energy, the wave height of the leading tsunami became smaller as it reached the Hawaiian Islands chain; the wave height was about 2m. However, due to shoaling and focusing effects, a significant inundation occurred at Hilo Bay.

The smallest grid size is 5min (approximately 9km) of latitude by 5min (approximately 9km) of longitude in the ETOPO5. In the linear model, the largest grid is 10min(approximately 18.5km), whereas the smallest is 11.1sec(approximately 342m). The detailed bathymetric data near the Hawaiian Islands chain and inside Hilo Bay are obtained through digitization of more detailed local maps.

Computed free surface displacements are first shown at several locations in the Pacific Ocean. The coastlines of the Pacific Ocean are shown in Fig. 1. Locations where the free surface displacements are computed are also

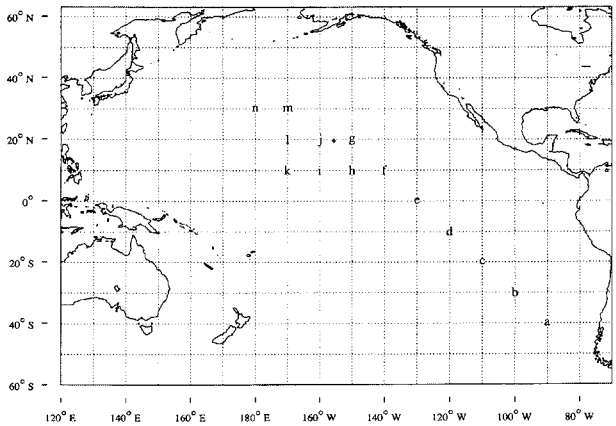

Fig. 1. Locations where time histories of free surface profiles are computed

displayed in Fig. 1, while time histories of free surface displacements at locations (a)-(n) are plotted in Fig. 2. In the figure, at location (a) near the source region, the leading wave appears to be a solitary wave followed by a relatively wide trough negative wave. As tsunamis propagate into the Pacific Ocean, the wave front spreads over a large area, reducing the leading wave amplitude(unit: m). Because of the frequency dispersion, the leading wave evolves into two positive waves between location (b) to location (g), and the negative wave becomes shorter with a large amplitude. The station (j) is located in the vicinity of Hawaii Island. The leading wave arrives approximately 14 hours later, while the peak arrives approximately 15 hours after the leading wave. The high frequency oscillations are amplified during the ocean journey.

4. Numerical Simulation of Run-up Process

To estimate the maximum inundation area inside Hilo Bay, a grid system with a 100m by 100m mesh is used to cover an area of 9.9km wide and 16.0km long. Although the inundation

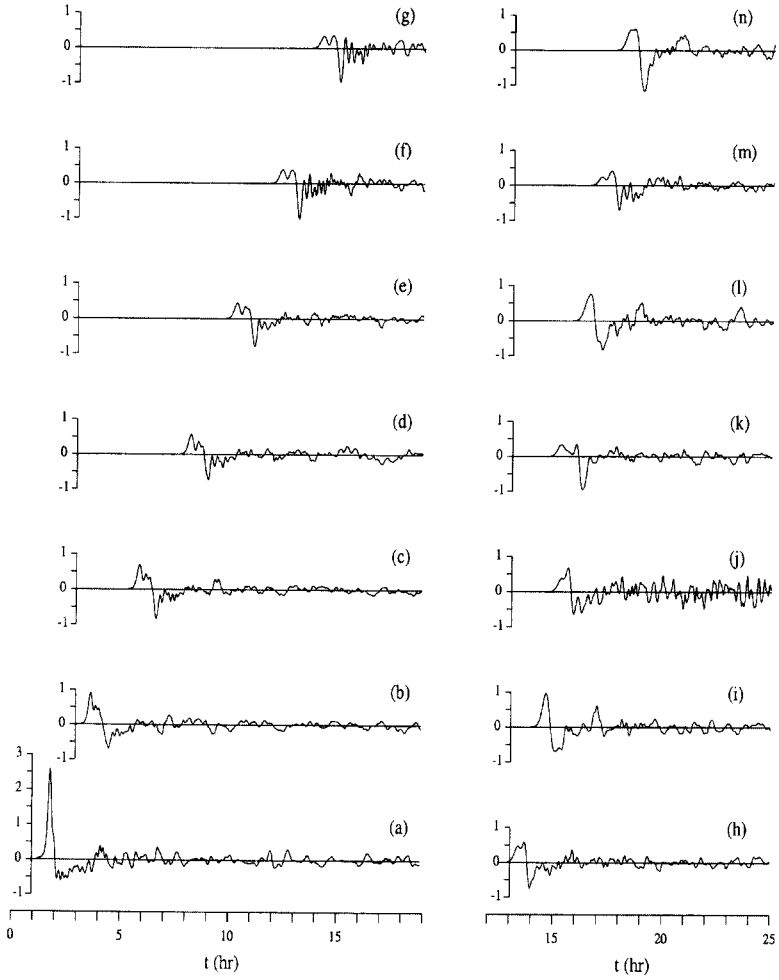

Fig. 2. Time histories of free surface profiles at locations (a)-(n)

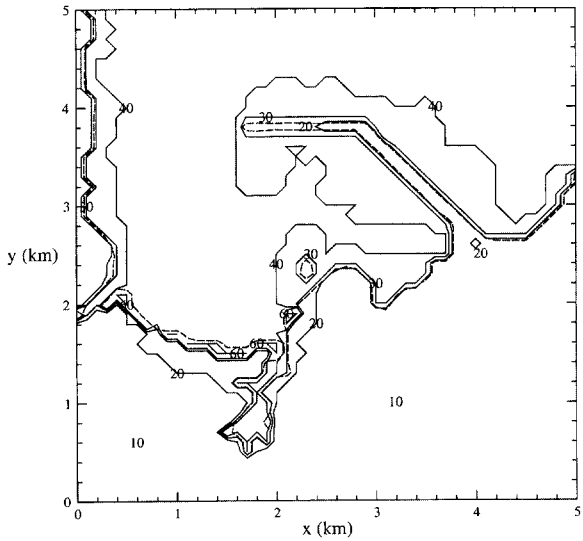

Fig. 3. Variable Chezy's friction coefficients of Hilo Bay, Hawaii

model covers an area of 9.9km wide and 16.0km long, a 5km by 5km area is only shown in figures to be followed.

Both the bathymetry of the Bay and the land topography are digitized and stored for each mesh. Although not plotted in Fig. 3, the boundary conditions along the offshore(x direction) and lateral(y direction) boundaries are time series of free surface displacements obtained from the transoceanic propagation model. A linear interpolation is used to transfer the information. Since the smallest grid size of the linear model is 342m, 30 grids along the offshore boundary and 48 grids (including 8 grids on the land) along the lateral boundary are used. A moving boundary condition is implemented along the shoreline to track the transient movement of shoreline and a radiation boundary condition is specified along the offshore and lateral boundaries (Liu et al., 1995).

The maximum inundation area at Hilo Bay is calculated by using variable Chezy's frictional coefficients. Fig. 3 displays variable Chezy's frictional coefficients obtained from the Look Laboratory of University of Hawaii(Mader and Curtis, 1991).

The maximum inundation area is shown in Fig. 4. The field observation is also plotted for comparison. The present numerical model slightly overestimates the maximum inundation area comparing with the observed data. The over-prediction could be caused by the uncertainties in bottom friction coefficients and the reliability of the data in the source region. The spatial grid size is also too large to cover the complicated local geometry in detail. Despite these reasons, the overall agreement between the observed data and numerical solutions of the present model is encouraging. Following to Lander and Lockridge(1989), specially, the maximum inundation is roughly equal to the contour of 6m above the still water level. The maximum inundation line obtained from the present model approximately coincides with the contour of 6m.

Finally, numerical solutions of the maximum run-up heights are obtained at several locations and compared with the observed data and other numerical solutions as presented in

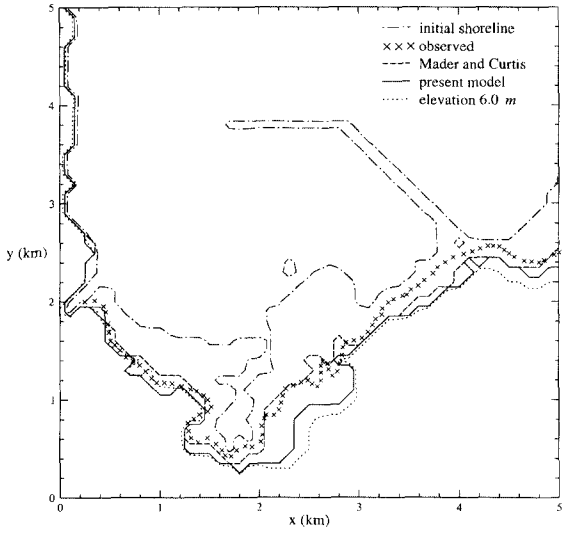

Fig. 4. Maximum inundation zones due to the 1960 Chilean tsunami

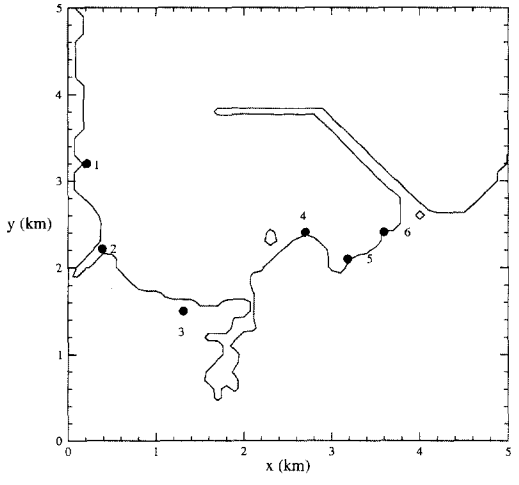

Fig. 5. Calculated free surface displacements at six locations: 1; Hilo Sugar Mill, 2; Wailuku bridge, 3; Theater, 4; Waiakea, 5;R eeds Bay, 6; Pier 2

Table 1. These locations are displayed in Fig. 5. Although overestimations occur at two locations, the overall agreement between the field observed data and the present predictions is found reasonably good. Look Laboratory represents the run-up heights obtained from the Look Laboratory model and the results are also shown in Table 1(Mader and Curtis, 1991).

5. Concluding Remarks

The transoceanic propagation across the Pacific Ocean and associated run-up process inside Hilo Bay of the 1960 Chilean tsunami are simulated numerically in this study. A composite of the transoceanic propagation and the inundation models based on the finite difference method is devised.

Table 1. Comparison of maximum run-up heights

location	observed (m)	Mader and Curtis (m)	Look Lab (m)	present (m)
Hilo Sugar Hill	4.6-6.1	3.7	6.7	5.7
Wailuku Bridge	4.3-5.8	4.5	3.8	5.9
Theater	6.7-8.5	4.5	7.6	6.2
Waiakea	4.6-6.1	4.2	3.5	5.4
Reeds Bay	2.7-3.7	4.9	4.1	5.9
Pier 2	3.6-4.3	5.0	4.4	5.9

The maximum inundation map inside Hilo Bay is generated and compared with field data. A resonable agreement is observed. This inundation map is almost identical with the topographic contour of 6m, which is the maximum inundation line reported by NOAA(Lander and Lockridge, 1989).

Although there is a slight discrepancy, the present model predicts the maximum run-up heights and inundation map reasonably agreeable to field recordings. The numerical model can be chosen as a plausible tool to plan a tsunami hazard mitigation. The obtained inundation map could be used by the authorized organizations to make evacuation plans against cases of real tsunami attacks.

Acknowledgements

This research was supported by Korea Science and Engineering Foundation research grant to Hanyang University(No. 1999-2-311-005-3).

References

Cho, Y.-S. (1995). *Numerical Simulations of Tsunami Propagation and Run-up*, Ph.D. Thesis, Cornell University, NY., USA.

Cho, Y.-S. and Liu, P.L.-F. (1999). "Crest length effects in nearshore tsunami run-up around islands," *Journal of Geophysical Research*, Vol. 104, pp. 7907~7913.

Cho, Y.-S. and Yoon, S.B. (1998). "A modified leap-frog scheme for linear shallow-water equations," *Coastal Engineering Journal*, Vol. 40, No. 2, pp. 191~205.

Houston, J.R. (1978). "Interaction of tsunamis with the Hawaiian islands calculated by a finite-element numerical model," *Journal of Physical Oceanography*, Vol. 8, pp. 93~102.

Imamura, F., Shuto, N. and Goto, C. (1988). "Numerical simulations of the transoceanic propagation of tsunamis," *Proceedings of 6th Congress Asian and Pacific Regional Division*, Japan, pp. 265~272.

Kajiura, K. and Shuto, N. (1990). "Tsunami," in The Sea, edited by B. Le Mehaute, and D.M. Hanes, Vol. 9, Part B, John Wiley & Sons, Inc.

Lander, J.F. and Lockridge, P.A., (1989). *United States Tsunamis*, pp. 265, U.S. Department of Commerce.

Liu, P.L.-F., Cho, Y.-S., Briggs, M.J., Synolakis, C.E. and Kanoglu, U. (1995). "Run-up of solitary wave on a circular island," *Journal of Fluid Mechanics*, Vol. 302, pp. 259~285.

Mader, C.L. and Curtis, G.D. (1991). *Numerical Modeling of Tsunami Inundation of Hilo Harbor*, JIMAR Contribution No. 91-251, University of Hawaii, Honolulu.

Manshiha, L. and Smylie, D.E. (1971). "The displacement fields of inclined faults," *Bulletin of the Seismological Society of America*, Vol. 61, pp. 1433~1440.

(논문번호:00-075/접수:2000.12.30/심사완료:2001.03.29)